Swanirman Sunirmit Publications of Research - 7th ICRTTEAS July 2025 | [2025-26]
ISSN [Online]: 2583-2654

Axial Ratio Bandwidth Enhancement of DBDCP Fabry–Pérot Cavity Antenna for Vehicular MIMO Communications and Sensing

Dr Jenitha A, Pramod S, Stephen Prashanth C,
Department of ECE, Dr. T. Thimmaiah Institute of Technology

Abstract: This article presents a dual-band dual-circularly polarized (DBDCP) MIMO antenna with enhanced axial ratio (AR) bandwidth using a novel polarization-independent partial reflective surface (PRS). The PRS unit cell features two metallic patterns—C-shaped arcs and circular patches—rotated 90° on opposite substrate surfaces. It converts linearly polarized waves into circularly polarized (CP) waves across two bands. A Fabry-Pérot cavity (FPC) enables simultaneous x- and y-polarized wave generation, leading to a wide AR bandwidth. A prototype was fabricated and tested, achieving VSWR < 2 from 11.55–14.8 GHz, with LHCP and RHCP in 12–12.6 GHz and 14.1–14.61 GHz bands, respectively. The antenna shows high gain (up to 13.5 dBi) and low ECC, suitable for Ku-band vehicular MIMO applications.

Keywords: ***Dual-band circularly polarized antenna, Partial reflective surface (PRS), IoT, Vehicular MIMO communication***

I. INTRODUCTION

Multiple-input multiple-output (MIMO) technology has proven effective in enhancing data rates, improving channel capacity, and reducing latency in multipath environments. It has become a foundational element in modern wireless communication systems. In satellite MIMO communications, antennas with circular polarization (CP) operating at dual frequency bands are particularly advantageous. CP antennas minimize polarization mismatch, mitigate multipath fading, and offer better penetration. Moreover, a dual-band dual-circularly polarized (DBDCP) antenna enables full-duplex communication—using left-hand circular polarization (LHCP) in the uplink (e.g., 12–12.5 GHz) and right-hand circular polarization (RHCP) in the downlink (e.g., 14–15 GHz) within the Ku-band.

This dual functionality enhances the efficiency and reliability of satellite communications, making the realization of a DBDCP MIMO antenna a topic of strong interest. Prior research has explored different approaches to achieve DBDCP performance. For instance, an antenna employing a 45° rotating ellipse-shaped patch as the unit cell in a frequency-selective surface (FSS) was able to reach axial ratio (AR) bandwidths of 3% and 4.1%. Another study used a reflect array (RA) composed of dual-ring elements with hybrid rotating branches, achieving AR bandwidths of 26.4% in K-band and 24.6% in Ka-band. However, other conventional patch-based methods, using orthogonal modes like TM10/TM01 and TM30/TM03, demonstrated very narrow AR bandwidths of 0.67% and 0.6%.

Other designs using antenna arrays for DBDCP applications also suffered from limited AR bandwidth. Recent research has focused on chiral metamaterials (CMMs) for their polarization conversion capabilities, utilizing structures like twisted arcs and U-shaped resonators with square patches at a 90° orientation. These designs leverage circular dichroism and optical rotation to enhance AR bandwidth. Additionally, artificial magnetic conductors (AMCs) with polarization rotation properties have shown promise. For example, one design achieved AR bandwidths of 2% and 8.2%, with peak gains of 6.6 dBi and 7.2 dBi at the respective bands.

Despite these advancements, many existing DBDCP antenna designs still face challenges in achieving wide AR bandwidth, high gain, and low

ISSN [Online]: 2583-2654

complexity. Therefore, the development of a high-performance DBDCP MIMO antenna that balances wide AR bandwidth, robust polarization diversity, and practical fabrication remains a key objective in advancing satellite and vehicular communication technologies, especially in the Ku-band spectrum.

II. METHODOLOGY

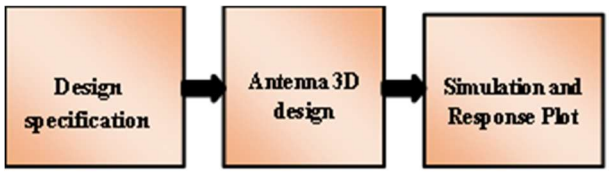

Fig 1: Block diagram of circular patch

When designing an electromagnetic component like an antenna using HFSS software, it is crucial to define comprehensive design specifications that guide the entire process. These specifications include key parameters such as operating frequency, bandwidth, polarization, gain, directivity, and impedance matching, which influence the geometry, material properties, and simulation settings. For patch antennas, specific details like patch dimensions, substrate material properties, and feed mechanisms are essential. The 3D design process begins with defining the antenna's geometry based on the desired frequency and radiation characteristics, followed by selecting suitable conductive materials and determining the appropriate feed point location. Electromagnetic simulation tools such as HFSS are then used to analyze critical performance aspects including impedance matching, radiation patterns, and gain. Optimization techniques help fine-tune these parameters to meet performance goals, after which a prototype can be fabricated for testing and validation. CAD tools assist in visualizing and refining the antenna structure during this phase. Simulation results are typically presented as stimulation and response plots. Stimulation plots include the radiation pattern, which shows energy distribution in space, VSWR to assess impedance matching, and impedance plots. Response plots provide return loss (measuring reflected power), gain (ability to focus energy), and directivity (power concentration in a specific direction), all of which help validate the antenna's effectiveness.

Additionally, accurate meshing and boundary condition setup in HFSS are essential to ensure simulation precision. The mesh must be fine enough to capture the physical details of the antenna without excessively increasing computation time. Proper boundary conditions, such as radiation boundaries or perfect electric conductors (PEC), must be applied to replicate real-world scenarios. Furthermore, port excitation settings like lumped ports or wave ports must be appropriately configured for reliable S-parameter extraction. Time and frequency domain analyses can be conducted to observe behavior under varying signal conditions. The post-processing stage involves evaluating results and comparing them with the target specifications. If discrepancies exist, iterative tuning of design parameters is performed until optimal performance is achieved.

III. IMPLEMENTATION

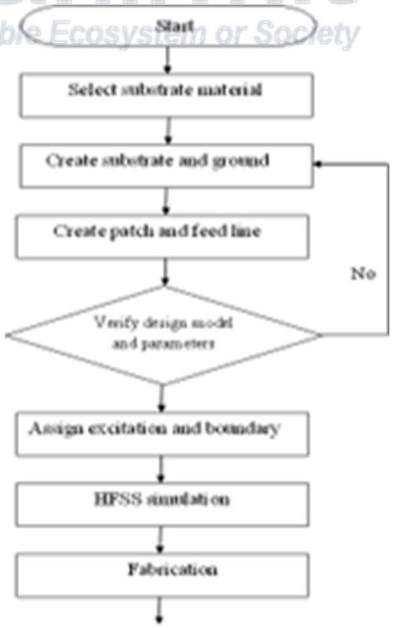

Fig 2: Flow chart

The implementation process involves selecting the substrate, designing the ground, patch, and feed line, verifying parameters, assigning excitation and

ISSN [Online]: 2583-2654

boundaries, simulating in HFSS, and finally fabricating the antenna. The simulated rectangular patch antenna is shown with front and back views, illustrating its basic structural design.

IV. DETAILS OF EMERGENCY TYPE

(i). Type-1: Communication Stability During Accidents In vehicular accidents, reliable antenna performance ensures uninterrupted transmission of emergency data such as location, sensor readings, and alerts. Dual-band circular polarization helps maintain link quality under dynamic vehicle orientation.

(ii). Type-2: Health and Safety Monitoring
The antenna enables robust MIMO links for transmitting real-time data from health or safety monitoring sensors. Enhanced AR bandwidth ensures consistent performance even in dense or reflective environments.

(iii). Type-3: Surveillance and Criminal Emergency Response During criminal incidents or security breaches, real-time video or sensor data can be streamed via MIMO systems. The proposed antenna maintains strong, low-interference communication links needed for rapid response and situational awareness.

(iv) Type-4: Environmental Hazard Detection The antenna enables the vehicle to detect and communicate environmental hazards, such as landslides, floods, or fires. Real-time alerts are transmitted to emergency services and nearby vehicles, ensuring swift evacuation or assistance.

(v)Type-5: vehicle system failures the system monitors the vehicle's internal components, detecting mechanical or electrical failures. Upon detection, the antenna facilitates the transmission of fault data to maintenance teams or control centers, allowing for quicker repairs and minimizing downtime.

V. RESULT ANALYSIS

The result analysis of the proposed DBDCP Fabry–Pérot cavity MIMO antenna shows significant performance improvements for vehicular communication. The antenna achieves dual-band circular polarization with wide axial ratio (AR) bandwidths of 4.88% (12–12.6 GHz) and 3.55% (14.1–14.61 GHz). The measured gain peaks at 13.5 dBi (low band) and 14.1 dBi (high band), with excellent port isolation above 48 dB and extremely low envelope correlation coefficients (ECC) of less than −80 dB and −107 dB, respectively. The antenna maintains stable unidirectional radiation even when mounted on a vehicle roof. Overall, the prototype demonstrates strong agreement between simulated and measured results, validating its high performance for Ku-band MIMO applications.

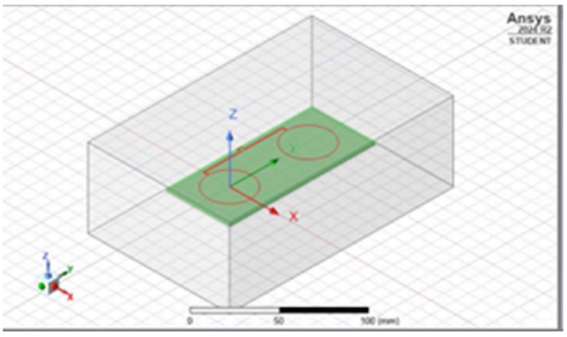

Fig 3: Final Antenna Design

To design the DBDCP Fabry–Pérot Cavity Antenna in HFSS, start by creating a new project and defining the substrate material (e.g., FR4). Design dual C-shaped arcs and circular patches rotated 90° on opposite sides of the substrate to enable dual-band circular polarization (LHCP and RHCP). Incorporate a Fabry-Pérot cavity (FPC) structure with a polarization-independent partial reflective surface (PRS) for enhanced AR performance. Apply a microstrip feed to excite the antenna. Simulate the design, focusing on axial ratio (AR), gain, and bandwidth. Optimize the patch size, cavity dimensions, and substrate thickness to achieve the desired AR bandwidth.

Finally, analyze the performance through S-parameters and radiation patterns.

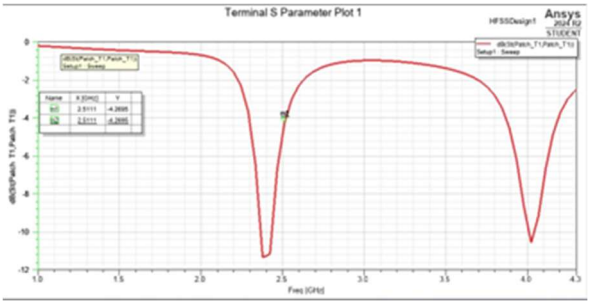

Fig 4: S 11 Parameter

ISSN [Online]: 2583-2654

The S11 parameter indicates how much input power is reflected from the antenna. For a dual-band antenna operating at 2.45 GHz and 4.0 GHz, achieving S11 below –10 dB at both frequencies confirms efficient impedance matching. This ensures minimal power loss, enabling reliable performance for wireless communication across both targeted bands.

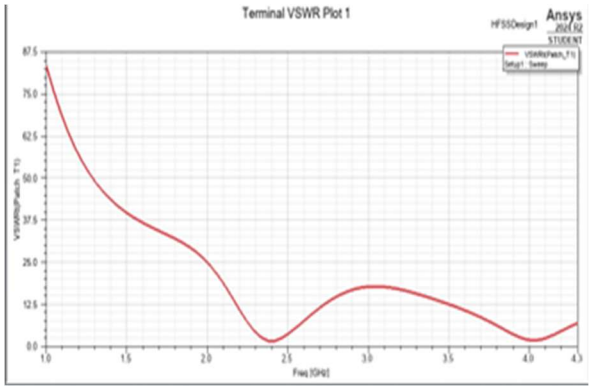

Fig 5: VSWR output

The Voltage Standing Wave Ratio (VSWR) measures how efficiently radio-frequency power is transmitted from a source to a load, such as an antenna. For a dual-band antenna operating at 2.45 GHz and 4.0 GHz, a VSWR value close to 1:1 indicates excellent impedance matching. Typically, a VSWR less than 2:1 is acceptable, meaning minimal power is reflected back. At 2.45 GHz and 4.0 GHz, achieving VSWR values under 2 ensures effective signal transmission with reduced losses, essential for applications like Wi-Fi, Bluetooth, or IoT. Proper VSWR across both bands guarantees optimal antenna performance and reliable wireless communication in dual-frequency environments.

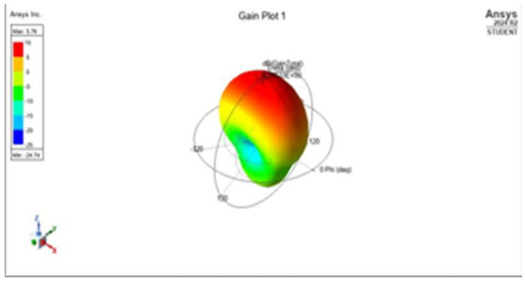

Fig 6: Gain

Antenna gain is a critical parameter that indicates how effectively an antenna converts input power into radio waves in a specific direction. It combines both the antenna's efficiency and directivity. Measured in decibels (dBi), higher gain values suggest stronger signal transmission and reception in the intended direction. For dual-band antennas operating at 2.45 GHz and 4.0 GHz, maintaining consistent gain across both bands is essential for reliable performance. In practical applications such as wireless communication, IoT, or vehicular systems, a gain of 2–9 dBi is typically desirable depending on the coverage and range required.

Antennas with higher gain focus energy more narrowly, ideal for long-distance or directional communication. However, excessively high gain can reduce coverage area, making balance important. During antenna design and testing in tools like HFSS, gain is analyzed alongside parameters like VSWR and S11 to ensure optimal system performance. Ultimately, gain reflects an antenna's real-world ability to strengthen wireless connectivity.

Additionally, gain directly influences battery efficiency in portable devices by reducing retransmissions. A well-optimized gain pattern ensures signal strength even in multipath or obstructed environments. For MIMO and smart antenna systems, consistent gain across all elements improves diversity and throughput, making gain a vital factor in next-generation wireless system designs.

Directivity is a fundamental parameter in antenna design that measures how concentrated an antenna's radiation pattern is in a particular direction. It quantifies the ability of an antenna to focus energy in one direction as opposed to spreading it equally in all directions, like an isotropic radiator. Directivity is expressed in decibels (dBi) and is independent of the antenna's efficiency.

A high-directivity antenna radiates more power in a specific direction, making it ideal for long-range

ISSN [Online]: 2583-2654

communication or targeted signal transmission, such as in satellite, radar, or point-to-point wireless systems.

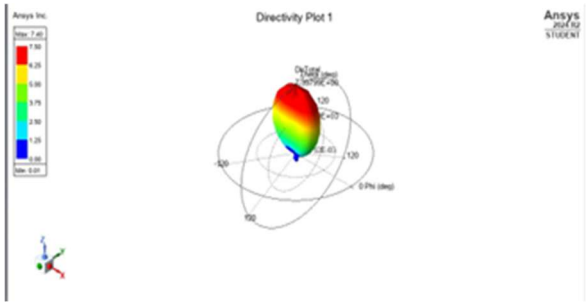

Fig 7: Directivity

In applications such as vehicular communications and MIMO systems, antennas with moderate directivity are preferred to ensure both sufficient range and wide coverage. For directional antennas, such as those designed with Fabry–Pérot cavities or reflector structures, directivity is carefully optimized using simulation tools like HFSS. Unlike gain, which accounts for losses, directivity focuses solely on the shape and strength of the radiation pattern. Higher directivity improves signal strength in the desired path but may reduce performance in off-axis directions.

Understanding directivity helps in balancing coverage and performance based on the application—broad coverage for mobile systems or focused beams for high-speed data links. It is crucial for designing efficient, purpose-driven antenna systems.

VI. CONCLUSION

The proposed dual-band dual-circularly polarized (DBDCP) Fabry–Pérot cavity antenna effectively enhances axial ratio (AR) bandwidth while maintaining high gain and low envelope correlation, making it highly suitable for vehicular MIMO communications and sensing in the Ku-band. By employing a polarization-independent partial reflective surface (PRS) with symmetric C-shaped arcs and circular patches, the antenna achieves reliable LHCP and RHCP performance across two frequency bands. The improved AR bandwidth ensures robust circular polarization, reducing signal degradation in dynamic vehicular environments. Simulated and measured results validate the antenna's efficiency, with gains exceeding 13 dBi and excellent port isolation, supporting high data rates and stable connectivity. The antenna's design not only addresses multipath fading but also enhances directional communication essential for smart transportation systems. This advancement offers a promising solution for future intelligent vehicular networks requiring efficient dual-band operation and strong polarization performance.

REFERENCES

[1] W. Wang and Y. Zheng, "Wideband gain enhancement of high-isolation Fabry-Perot antenna array with tandem circular parasitic patches and radial gradient PRS," IEEE Trans. Antennas Protag., vol. 69, no. 11, pp. 7959–7964, Nov. 2021.

[2] W. Wang, S. Yang, Z. Fang, Q. Sun, Y. Chen, and Y. Zheng, "Compact dual-polarized wideband antenna with dual-/single-band shifting for micro base station applications," IEEE Trans. Antennas Protag., vol. 69, no. 11, pp. 7323–7332, Nov. 2021.

[3] S. Yang and L. Hanzo, "Fifty years of MIMO detection: The road to large-scale MIMOs," IEEE Commun. Surveys Tuts., vol. 17, no. 4, pp. 1941–1988, Fourth quarter 2015.

[4] X. Chen, P. Wang, Y. Shao, and H. Jin, "Gradient relative permittivity superstrate for decoupling of two closely located dual-polarized slot antennas," IEEE Trans. Antennas Protag., vol. 70, no. 4, pp. 3046–3051, Apr. 2022.

[5] F. Ferrero, C. Luxey, G. Jacque mod, and R. Stara, "Dual-band circularly polarized microstrip antenna for satellite applications," IEEE Antennas Wireless Protag. Lett., vol. 4, pp. 13–15, 2005.

[6]. N. Divya, P. Vijay, T. Yaswanth, U. Lokesh, and T. Venu, "RF and IoT-Driven Automated Lane Clearance System for Enhanced Emergency Response,

[6] J. Zhu, Y. Yang, S. Li, S. Liao, and Q. Xue, "Dual-band dual-circularly polarized antenna array using FSS-integrated polarization rotation AMC ground for vehicle satellite communications," IEEE Trans. Veh. Technol., vol. 68, no. 11, pp. 10742–10751, Nov. 2019.

[7] R. L. Farias, C. Pineiro, and M. V. T. Heckler, "Single-layer dual-band dual-circularly polarized reflect array for space communication," IEEE Trans. Antennas Protag., vol. 70, no. 7, pp. 5989–5994, Jul. 2022.

[8] J.-D. Zhang, L. Zhu, N.-W. Liu, and W. Wu, "Dual-band and dual circularly polarized single-layer microstrip array based on Mult resonant modes," IEEE Trans. Antennas Protag., vol. 65, no. 3, pp. 1428–1433 Mar. 2017.

[9] Q.-S. Wu, X. Zhang, L. Zhu, J. Wang, G. Zhang, and C.-B. Guo, "single-layer dual-band dual-sense circularly-polarized patch antenna array with small frequency ratio," IEEE Trans. Antennas Protag., vol. 70, no. 4 pp. 2668–2675, Apr. 2022.

[10] C. Zhu, G. Xu, A. Ren, W. Wang, Z. Huang, and X. Wu, "A compact dual-band dual-circularly polarized SIW cavity-backed antenna array for millimeter-wave applications," IEEE Antennas Wireless Protag. Lett. vol. 21,

ISSN [Online]: 2583-2654

no. 8, pp. 1572–1576, Aug. 2022.

[11] X. Ma, C. Huang, W. Pan, B. Zhao, J. Cui, and X. Luo, "A dual circularly polarized horn antenna in Ku-band based on chiral metamaterial," IEEE Trans. Antennas Protag., vol. 62, no. 4, pp. 2307–2311, Apr. 2014.

[12] C. Chen, Z.-G. Liu, H. Wang, and Y. Guo, "Metamaterial-inspired self-polarizing dual-band dual-orthogonal circularly polarized Fabry-Pero resonator antennas," IEEE Trans. Antennas Protag., vol. 67, no. 2, pp. 1329–1334, Feb. 2019.

[13] H. Yang, X. Liu, Y. Fan, and L. Xiong, "Dual-band textile antenna with dual circular polarizations using polarization rotation AMC for off-body communications," IEEE Trans. Antennas Protag., vol. 70, no. 6, pp. 4189–4199, Jun. 2022.

[14] T. Yue, Z. H. Jiang, and D. H. Werner, "A compact meta surface-enable dual-band dual-circularly-polarized antenna loaded with complementary split ring resonators," IEEE Trans. Antennas Protag., vol. 67, no. 2, pp. 794–803, Feb. 2019.

[15]P.Wang,J.Liu,C.Zhou,B.Yin,andW.Wang,"Dual-banddual-circularly polarized Fabry-Perot cavity MIMO antenna using CMM-based polarization converter and MMA for vehicular satellite communications," IEEE Trans. Veh. Technol., vol. 72, no. 7, pp. 8844–8856, Jul. 2023